JOURNAL OF Materials CHEMISTRY

FTIR study of the thermal transformation of barium-exchanged zeolite A to celsian

Antonio Aronne,*[a] Serena Esposito,[b] Claudio Ferone,[b] Michele Pansini[b] and Pasquale Pernice[a]

[a]*Dipartimento di Ingegneria dei Materiali e della Produzione, Università di Napoli Federico II—Piazzale Tecchio 80, 80125 Napoli, Italy*
[b]*Laboratorio Materiali del Dipartimento di Meccanica, Strutture, Ambiente e Territorio, Facoltà di Ingegneria dell'Università di Cassino, Via G. Di Biasio 43, 03043 Cassino (Fr), Italy*

Received 22nd April 2002, Accepted 17th June 2002
First published as an Advance Article on the web 16th August 2002

In this study room temperature X-ray diffraction patterns and FTIR spectra of zeolite A in its Na form, Ba-exchanged zeolite A, hexacelsian, monoclinic celsian and Ba-exchanged zeolite A samples thermally treated at temperatures ranging from 200 to 1000 °C are reported. The combined inspection of room temperature X-ray diffraction patterns and FTIR spectra reveals the following points. 1) The thermal collapse of the microporous zeolite structure goes to completion upon thermal treatment at 200–300 °C; in the resulting amorphous phase the presence of the secondary building units of the zeolite A structure may be detected. 2) Thermal treatment in the temperature range 200–400 °C results in a middle-range order which favours the crystallisation of small crystallites of monoclinic celsian at 500 °C. 3) The further evolution of the amorphous phase in the 500–800 °C temperature range of thermal treatment instead of promoting the crystalline growth of monoclinic celsian, creates a middle-range order favourable to the crystallisation of hexacelsian which occurs at 1000 °C.

1 Introduction

Monoclinic celsian ($BaAl_2Si_2O_8$) is used as a refractory, high temperature electrical insulator, or as substrates for integrated circuits on account of its good thermal and electrical properties.[1] Moreover fibre-reinforced, monoclinic celsian matrix composites are being developed as viable candidate materials for high temperature structural applications in the aeronautic and aerospace fields.[2–9]

The synthesis of monoclinic celsian causes considerable problems.[10] On the one hand it requires high temperatures and/or long reaction times, which gives rise to high process costs. On the other hand the first polymorph to nucleate is hexagonal celsian (hexacelsian) even if it is stable at temperatures higher than 1590 °C.[11] This behaviour was ascribed to the simpler crystal structure of the high symmetry modification presenting a lower kinetic barrier to nucleation.[12]

The early crystallisation of hexacelsian appears to be a serious drawback on account of two reasons. On the one hand hexacelsian cannot be used as a refractory because, at 300 °C, it undergoes a reversible transformation into an orthorhombic form accompanied by a detrimental ($\geqslant 3\%$) volume change.[11] On the other hand the transformation of hexacelsian to monoclinic celsian occurs after prolonged heating (more than 20 hours) at temperatures higher than 1500 °C in the presence of mineralizers and monoclinic seed particles.[13]

The technique proposed by Subramanian and coworkers[14–17] for the synthesis of alkaline-earth and alkaline framework aluminosilicates, belonging to the class of feldspars, appeared proper for the synthesis of celsian. These authors crystallised such materials thermally, by treating various zeolites previously subjected to alkaline-earth or alkaline cation exchange at temperatures slightly higher than 1000 °C for some hours. This thermal treatment gave rise to the thermal collapse of the microporous zeolitic structure with the formation of an amorphous phase and, subsequently, to the crystallisation of the corresponding alkaline-earth or alkaline feldspar. The main advantages arising from this technique are the following: 1) the desired starting composition of the system may be easily reproduced by selecting zeolites exhibiting the required Si : Al ratio[18] and by properly adjusting the cation exchange operations; 2) the perfect homogeneity of composition on an atomic scale of the amorphous phase arising from the thermal collapse of the microporous zeolitic structure; 3) the low cost of many zeolitic substrates which may act as starting materials.

The technique proposed by Subramanian and coworkers[14–17] was successfully applied to the synthesis of monoclinic celsian starting from barium-exchanged zeolite A precursors.[10,19] Actually, it was found that, upon thermal treatment at 1100 °C, Ba-exchanged zeolite A, which after dehydration exactly reproduces the stoichiometric composition of celsian, gave rise to the following sequence of transformations: zeolite→amorphous phase→hexacelsian→monoclinic celsian. Moreover it was found that 6 hours of this treatment were sufficient to transform a sample of Ba-exchanged zeolite A, containing 0.60 meq g^{-1} Na residual content, into fully monoclinic celsian.

The very high reactivity of barium-exchanged zeolite A precursors was partially ascribed to its residual Na content.[19] Actually a higher value of this quantity was found to result in lower temperatures and times of transformation, *ceteris paribus*.[19]

Nevertheless the residual Na content alone does not appear sufficient to explain the very high reactivity of Ba-exchanged zeolite precursors. Actually, thermal treatment at 1300 °C for 22 hours of a sample of zeolite A subjected to exhaustive Ba-exchange (0.20 meq g^{-1} Na residual content) was found sufficient to fully convert it into monoclinic celsian.[19] The same result was obtained by Hoghooghi and coworkers[13] starting from Ba-exchanged zeolite X only by thermal treatment at 1550 °C for 24 hours.

Possible further explanations of the very high reactivity of Ba-exchanged zeolite A precursors could be found by characterising the amorphous phase arising from the thermal collapse of the microporous zeolitic structure and the early stage of the crystallisation process, in which the presence of

small crystalline aggregates of monoclinic celsian dispersed in this amorphous phase was recorded,[19] by Fourier transform infrared (FTIR) spectroscopy. In particular this technique is used in this study to correlate the thermal transformations occurring upon heating Ba-exchanged zeolite A with both the short- and the middle-range order present in the amorphous phase arising from the thermal collapse of the microporous zeolitic structure.

2 Experimental

The Ba-exchanged zeolite A sample was prepared according to the following procedures. Carlo Erba reagent-grade synthetic zeolite 4A ($Na_{12}Al_{12}Si_{12}O_{48}\cdot 27H_2O$) was added to a warm (60–70 °C) Ba^{2+} (0.2 N) solution with a solid : liquid weight ratio (S : L) = 1 : 25 and left to stand overnight. The solution was prepared using bidistilled water and Carlo Erba reagent-grade $Ba(NO_3)_2$ (purity 99.5%). The solid was separated from the liquid by filtration and again added to the exchange solution for a total of four times. Then a fifth exchange was performed with S : L = 1 : 50, all other conditions being equal to the previous ones. The remaining exchange operations were performed contacting the zeolite with barium solutions prepared using extremely pure $BaCl_2$ (purity > 99.999%) provided by Aldrich. In particular a sixth exchange was performed with S : L = 1 : 20 and $[Ba^{2+}] = 0.5$ g dm^{-3}, a seventh with S : L = 1 : 30 and $[Ba^{2+}] = 7.5$ g dm^{-3}, and an eighth with S : L = 1 : 40 and $[Ba^{2+}] = 7.5$ g dm^{-3}, all other conditions being equal to the previous ones. The initial pH of the salt solutions used for the exchanges is about 5.8.

The residual Na content of zeolite A at the end of the exchange procedure was determined to be 0.20 meq g^{-1} according to the following procedure. The zeolite was chemically dissolved in a hydrofluoric and perchloric acid solution and its Na^+ concentration was determined by atomic absorption spectrophotometry (AAS), using a Perkin-Elmer Analyst 100 apparatus. The consistency of the concentration measurements used in the cation exchange operations was checked by determining the Ba^{2+} concentration by titration with EDTA using erio T as the indicator and a NH_3/NH_4^+ solution at pH 10 as buffer.[20]

The resulting powders were washed with bidistilled water, dried overnight at 80 °C and stored for at least 3 days in an environment having about 50% relative humidity to allow water saturation of the zeolite.

Ba-exchanged zeolite A samples, obtained according to the procedure previously described, were subjected to various thermal treatments in a Lenton furnace, which ensured a stable temperature to within ±2 °C, using Al_2O_3 crucibles. The samples were heated at a rate of 10 °C min^{-1} up to 200, 300, 400, 500, 600, 700, 800 and 1000 °C and subsequently quenched in air.

The polycrystalline sample of hexacelsian was obtained by heating the Ba-exchanged zeolite A sample at a rate of 10 °C min^{-1} up to 1300 °C and then quenching it in air. The polycrystalline sample of monoclinic celsian was obtained by heating the Ba-exchanged zeolite A sample at a rate of 10 °C min^{-1} up to 1400 °C, keeping it at this temperature for 22 hours and then quenching it in air.

These products were characterized by XRD at room temperature using a Philips X'PERT diffractometer, Cu-Kα radiation, with collection of data between 20 and 40° 2θ, with a step width of 0.02° 2θ, and 1 s data collection per step.

The structure of the investigated samples was analysed by room temperature Fourier transform infrared spectroscopy (FTIR). FTIR absorption spectra were recorded in the 4000–400 cm^{-1} range using a Nicolet system, Nexus model, equipped with a DTGS KBr (deuterated triglycine sulfate with potassium bromide windows) detector. A spectral resolution of 2 cm^{-1} was chosen. 2.0 mg of each test sample was mixed with 200 mg of KBr in an agate mortar, and then pressed into 200 mg pellets of 13 mm diameter. The spectrum of each sample represents an average of 32 scans, which were normalised to the spectrum of the blank KBr pellet.

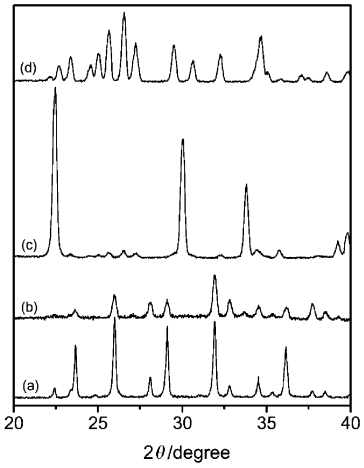

Fig. 1 XRD patterns of the zeolite Na-A (a), Ba-exchanged zeolite A (b), hexacelsian (c) and monoclinic celsian (d).

3 Results

3.1 X-Ray diffraction

In Fig. 1 are reported the XRD patterns of zeolite A in its Na (Na-A) (Fig. 1a) and Ba (Ba-A) (Fig. 1b) forms as well as the polycrystalline samples of hexacelsian (Fig. 1c) and monoclinic (Fig. 1d) celsian. It must be noticed that the XRD pattern of the sample of hexacelsian also reveals the presence of a small amount of monoclinic celsian. Actually it is reported in ref. 19 that it was not possible to obtain a sample of hexacelsian absolutely free from monoclinic celsian through the thermal transformation of Ba-exchanged zeolite.

XRD patterns of the Ba-exchanged zeolite A samples heated at different temperatures and then quenched in air are shown in Fig. 2. Although zeolite Ba-A heated at 200 °C (Fig. 2a)

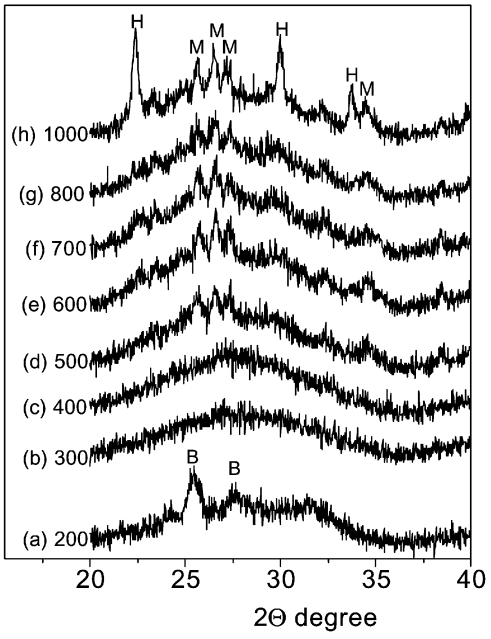

Fig. 2 XRD patterns of the Ba-exchanged zeolite A samples thermally treated at different temperatures. (a): 200 °C; (b): 300 °C; (c): 400 °C; (d): 500 °C; (e): 600 °C; (f): 700 °C; (g): 800 °C; (h): 1000 °C. B = banalsite, H = hexacelsian, M = monoclinic celsian.

appears to be almost completely amorphous, only two extremely broad diffraction peaks (denoted with B) are seen, which can be reasonably attributed to the presence of a small amount of the sodium–barium aluminosilicate banalsite, $BaNa_2Al_4Si_4O_{16}$, dispersed in the amorphous matrix. These extremely broad diffraction peaks disappear in the XRD patterns of samples thermally treated at 300 and 400 °C (Figs. 2b and 2c, respectively) which appear to be completely amorphous. In the XRD pattern of zeolite Ba-A heated at 500 °C (Fig. 2d) and then quenched in air, extremely broad diffraction peaks (denoted with M), which can be ascribed to monoclinic celsian, are observed. On raising the temperature of the thermal treatment to 600, 700 and 800 °C these peaks appear almost unchanged (Figs. 2e, 2f and 2g, respectively). In the XRD pattern of zeolite Ba-A heated at 1000 °C (Fig. 2h) and then quenched in air, diffraction peaks which can be ascribed to hexacelsian (denoted with H) are observed together with the same extremely broad diffraction peaks of monoclinic celsian recorded in Figs. 2d, 2e, 2f and 2g. Thus, at this stage, very small crystals of both celsian polymorphs are dispersed in the amorphous matrix of the sample.

3.2 Fourier transform infrared spectroscopy

Fig. 3 shows the following room temperature FTIR spectra: zeolite Na-A (Fig. 3a), Ba-exchanged zeolite A (Fig. 3b), polycrystalline sample of hexacelsian (Fig. 3c) and polycrystalline sample of monoclinic celsian (Fig. 3d).

The absorption bands present in these FTIR spectra were assigned on the basis of the results of previous papers and the assignments were related to the structure of the considered phases. The primary building units of the aluminosilicate framework are tetrahedra SiO_4 and AlO_4 which have four bridging oxygen atoms. Such tetrahedra are assembled in zeolite A so as to give rise to a structure characterized by a simple cubic cell in which eight truncated octahedral units (β cages), present at the corners of a cube, are connected by twelve double-4-ring units (D4R) present in the middle of the sides, thus enclosing a large cavity having the shape of a truncated cuboctahedron (α cage).[18,21] Moreover the electrostatic valence rule, as modified by Loewenstein, requires rigorous alternation of the SiO_4 and AlO_4 tetrahedra because the Si : Al ratio is equal to 1.[18] Therefore in the FTIR spectrum of zeolite Na-A (Fig. 3a) the main absorption band centred at 997 cm^{-1} is assigned to the stretching vibrations of the Si–O and Al–O bonds belonging to the SiO_4 and AlO_4 tetrahedra.[22–24] The corresponding internal bending modes of the Si–O–Al bonds give rise to the absorption band at 463 cm^{-1}.[23] Moreover two additional absorption bands were detected in the 500–800 cm^{-1} region: the first one at 668 cm^{-1} is broad and exhibits the lowest relative intensity whereas the second one occurs at 553 cm^{-1}. According to Mozgawa,[24] these bands can be assigned to the external vibrational modes of the tetrahedron rings producing the over-tetrahedral form of the zeolite middle-range order. In particular, since the zeolite A framework can be considered to be formed from single 6-membered rings (S6R) and double 4-membered rings (D4R),[21] the absorption bands at 668 and 553 cm^{-1} can be attributed to the vibration modes of the D4R and S6R units, respectively.

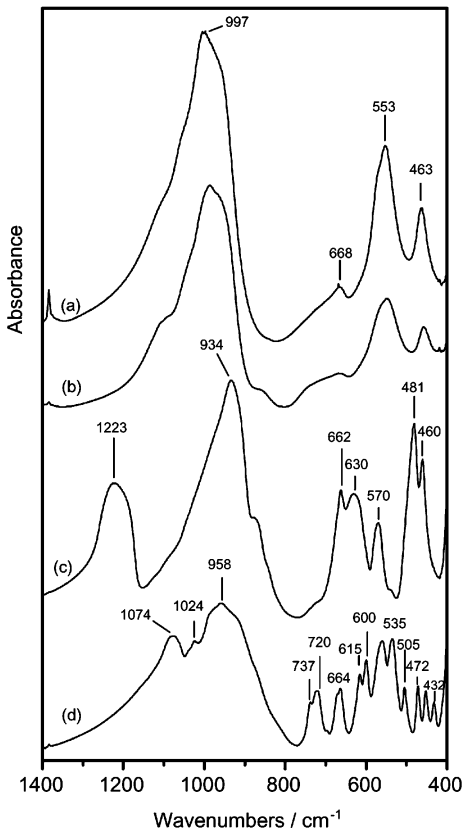

Fig. 3 FTIR spectra of the polycrystalline samples. (a): Zeolite Na-A; (b): Ba-exchanged zeolite A; (c) hexagonal celsian; (d): monoclinic celsian.

The FTIR spectrum of Ba-exchanged zeolite A (Fig. 3b) differs from the FTIR spectrum of zeolite Na-A (Fig. 3a) in the following ways: 1) the main absorption band exhibits two additional shoulders at 1100 and 855 cm^{-1}; 2) the broad band lying in the 640–800 cm^{-1} range exhibits a new shoulder at 750 cm^{-1}.

The structure of the hexagonal celsian can be considered to be a double layer of mica-like sheets held by the apexes of oxygen tetrahedra.[25] Barium atoms occupy the positions between such double layers and hold them together to form the three-dimensional framework of the crystals.[25] Therefore, according to the IR and Raman spectra of this phase reported by Scanu *et al.*,[26] the absorption bands centred at 934 and 1223 cm^{-1} may be ascribed to the intramolecular vibrations of AlO_4 and SiO_4 tetrahedra (stretching of the Al–O and Si–O bonds), whereas the absorption bands occurring in the 400–500 cm^{-1} region may be related to the bending modes of the Si–O–Al bonds[26] (Fig. 3c). Moreover three absorption bands were detected in the 500–800 cm^{-1} region which can be attributed to the characteristic Si–O and Al–O stretching of the rings forming the mica-like sheets.

The FTIR spectrum of monoclinic celsian (Fig. 3d) differs from that of the hexagonal polymorph by exhibiting a greater number of absorption bands as a consequence of the reduction in the degree of symmetry of the structure of this polymorph and is in complete agreement with the one shown in ref. 26.

In Figs. 4 and 5 the FTIR spectra of the Ba-exchanged zeolite A samples heated at different temperatures and then quenched in air are reported. As one would expect, the linewidth of the absorption bands of the polycrystalline samples are narrower and have a higher intensity than those of the thermally treated Ba-exchanged zeolite A samples on account of their amorphous or scarcely crystalline nature. In the range of wavenumbers (400–1400 cm^{-1}) examined, all the FTIR spectra of the thermally treated Ba-exchanged zeolite A samples exhibit a higher absorption band in the 800–1200 cm^{-1} region. Its linewidth increases with the temperature of the thermal treatment. It is noteworthy that in the FTIR spectra of the samples heated at temperatures up to 700 °C the higher absorption band is split into two bands with two different peaks. The first one occurs at the same wavenumber value (985 cm^{-1}) regardless of the temperature of the thermal treatment, whereas the position of the second one changes from 960 cm^{-1} (Fig. 4a) to 949 cm^{-1} (Fig. 5b) on increasing the temperature of thermal treatment from 200 to 700 °C.

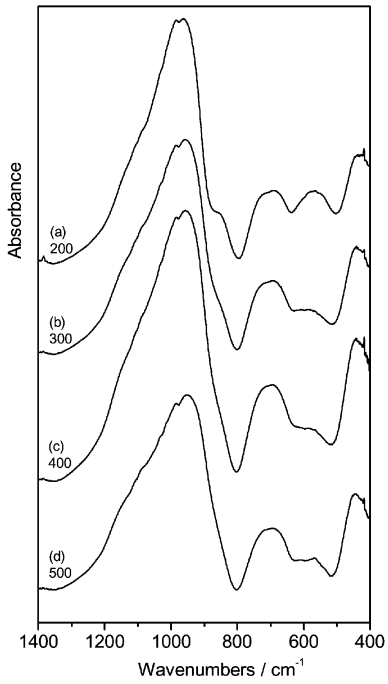

Fig. 4 FTIR spectra of Ba-exchanged zeolite A samples thermally treated at different temperatures. (a): 200 °C; (b): 300 °C; (c): 400 °C; (d): 500 °C.

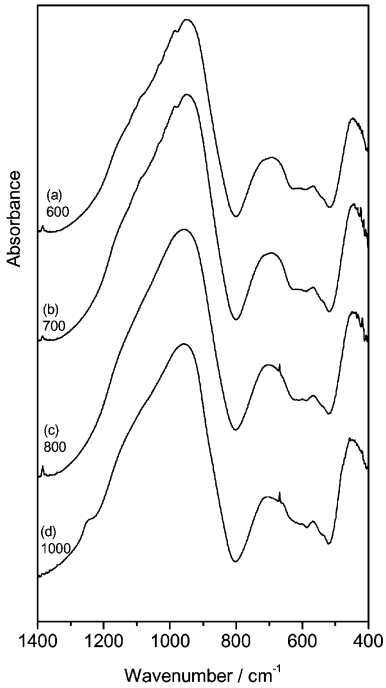

Fig. 5 FTIR spectra of Ba-exchanged zeolite A samples thermally treated at different temperatures. (a): 600 °C; (b): 700 °C; (c): 800 °C; (d): 1000 °C.

For the samples heated at 800 and 1000 °C and then quenched in air (Fig. 5c and 5d, respectively) the higher absorption band is centred at 960 and 956 cm^{-1}, respectively. Moreover, two absorption bands are evident in the 500–800 cm^{-1} region of the FTIR spectra of thermally treated samples of Ba-exchanged zeolite A. The intensity of the band occurring at the lower wavenumber dramatically decreases on increasing the temperature of the thermal treament of Ba-exchanged zeolite A from 200 to 500 °C (Fig. 4).

To understand the evolution with temperature of the FTIR spectra of the thermally treated samples as well as the structural modifications involved in the exchange procedure, curve fittings of the FTIR spectra of the Ba-exchanged zeolite A and of the thermally treated samples were performed using gaussian functions. The results are listed in Table 1. The peak fitting was carried out by non-linear least squares fitting based on the Levenberg–Marquardt algorithm.[27] In the curve fitting the

Table 1 Wavenumbers, $\tilde{\nu}$ (cm^{-1}), heights, A, estimated relative intensity, I, and full width at half maximum, Fw (cm^{-1}), computed from the peak fitting of the FTIR spectra of Ba-exchanged zeolite A and thermally treated samples of Ba-exchanged zeolite A

Zeolite A (Ba)				200 °C				300 °C				400 °C				500 °C			
$\tilde{\nu}$	A	I	Fw	$\tilde{\nu}$	A	I	Fw	$\tilde{\nu}$	A	I	Fw	$\tilde{\nu}$	A	I	Fw	$\tilde{\nu}$	A	I	Fw
1054	0.68	0.44	199	1050	0.63	0.57	226	1062	0.58	0.59	226	1070	0.72	0.59	222	1078	0.51	0.58	215
980	1.08	0.69	91	995	0.44	0.39	88	995	0.35	0.35	88	972	0.68	0.56	115	972	0.50	0.57	118
939	0.36	0.23	40	938	0.59	0.53	69	930	0.60	0.61	84	917	0.48	0.40	75	913	0.41	0.46	82
857	0.068	0.044	34	848	0.15	0.13	44	849	0.12	0.13	44	850	0.17	0.14	48	852	0.10	0.11	41
738	0.081	0.052	55	744	0.17	0.15	50	748	0.16	0.16	53	749	0.18	0.16	57	744	0.13	0.15	54
665	0.23	0.15	115	691	0.30	0.27	81	691	0.32	0.32	90	689	0.42	0.35	101	687	0.27	0.31	92
551	0.74	0.47	83	571	0.33	0.30	124	579	0.21	0.21	109	576	0.23	0.19	95	576	0.14	0.16	80
450	0.51	0.33	74	429	0.50	0.45	94	435	0.50	0.50	93	435	0.66	0.54	96	440	0.45	0.51	84
600 °C				700 °C				800 °C				1000 °C							
$\tilde{\nu}$	A	I	Fw	$\tilde{\nu}$	A	I	Fw	$\tilde{\nu}$	A	I	Fw	$\tilde{\nu}$	A	I	Fw				
1070	0.57	0.61	226	1086	0.63	0.59	211	1079	0.66	0.61	211	1200	0.21	0.20	265				
1009	0.13	0.13	84	999	0.32	0.30	111	1017	0.16	0.15	112	1059	0.66	0.61	213				
926	0.70	0.75	126	919	0.81	0.76	122	928	0.88	0.81	148	933	0.77	0.72	145				
—	—	—	—	—	—	—	—	—	—	—	—	—	—	—	—				
747	0.13	0.14	59	747	0.14	0.13	61	747	0.12	0.11	75	732	0.23	0.22	83				
685	0.32	0.34	104	685	0.37	0.34	106	686	0.45	0.42	130	658	0.34	0.32	124				
573	0.19	0.20	82	572	0.21	0.20	79	563	0.29	0.27	91	565	0.20	0.19	60				
442	0.51	0.54	89	442	0.60	0.56	88	447	0.71	0.66	88	444	0.67	0.63	106				

[a]800–1200 cm^{-1} stretching of the Si–O and Al–O bonds belonging to the SiO_4 and AlO_4 tetrahedra.
738–748 cm^{-1} vibrational modes of the simple four-membered ring (S4R) units.
665–691 cm^{-1} vibrational modes of the double four-membered ring (D4R) units.
551–576 cm^{-1} vibrational modes of the simple six—membered ring (S6R) units.
429–450 cm^{-1} bending internal modes of the Si–O–Al bonds.

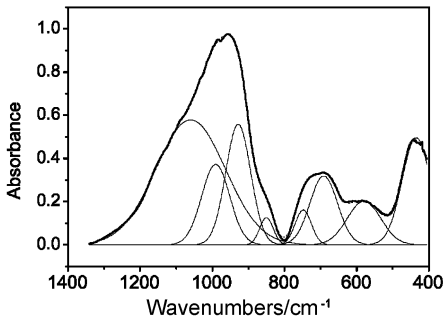

Fig. 6 Comparison of the experimental FTIR spectrum of the Ba-exchanged zeolite A sample heated at 300 °C and the calculated spectrum obtained by curve fitting using gaussian functions. The thin solid lines denote the individual peaks, the thick solid line, the experimental data, and the dotted line, the sum of the individual calculated peaks. The last two curves appear completely overlapped.

minimum number of gaussian functions was chosen to represent the FTIR spectrum. In connection with this, it is noteworthy that, according to Efimov,[28] the total number of bands can be estimated by consideration of the minimization of the error of the best fit and also by considering the physical meaning of each band, *i.e.* its relationship with a structural element in the framework. Usually errors arising from the determination of the gaussian parameters found in the fitting procedure were small, at less than 2%. A representative curve fit of the spectrum of the sample heated up to 300 °C and then quenched in air is also given in Fig. 6 and shows good agreement between the experimental and calculated spectra. Moreover, in order to compare the absorbance values of the different thermally treated samples, the ratio between the heights of the peaks of the gaussian function and the maximum absorbance value recorded for each FTIR spectrum is an estimate of the relative absorbance *I* (Table 1). Standard errors in the *I* values are less than 2%, based on the standard errors determined for the gaussian heights and widths.

4 Discussion

It is known that the symmetric and the anti-symmetric stretching modes of the Si–O bonds of the silica tetrahedron with *n* bridging oxygen atoms are IR active in the 800–1300 cm^{-1} region.[22] The absorption bands corresponding to values of *n* ranging from 4 to 0 occur at 1200, 1100, 950, 900 and 850 cm^{-1}, respectively. These values shift to lower wavenumbers on replacing the Si with Al atoms as a consequence of the weaker Al–O bond. Therefore, as the structure of zeolite A is formed by silicon and aluminium tetrahedra linked in turn through bridging oxygens, the main absorption band in their FTIR spectra is centred at a lower value (about 1000 cm^{-1}) than that expected for a SiO_4 tetrahedra framework.

The XRD diffraction patterns reported in Fig. 1 confirm that the exchange of $2Na^+$ with Ba^{2+} gives rise to a distortion in the framework and a subsequent loss of crystallinity in the zeolite.[19] These effects are more clearly revealed by the peak fitting analysis of the FTIR spectrum of the Ba-exchanged zeolite A based on an investigation by Smirnov and Bougeard.[29] Actually these authors calculated the IR spectrum of the zeolite Na-A and found the following characteristic absorption bands in the 400–1200 cm^{-1} range: 553, 581, 663, 936, 997, 1000 and 1051 cm^{-1}. The results concerning zeolite Ba-A (Table 1) are in very good agreement with Smirnov and Bougeard,[29] the only exceptions being the peaks at 857 and 738 cm^{-1}. Actually the peak at 738 cm^{-1} lies in the wavenumber range (500–800 cm^{-1}) where there are active pseudolattice vibrations, *i.e.* vibrations related to the rings forming the over-tetrahedral form of the zeolite middle-range order.[24] According to Mozgawa[24] the position of the ring bands is affected by several factors. Among them the most important are the number of ring members, the Si : Al ratio and the degree of ring deformation. In particular, the decrease in the number of ring members shifts the characteristic band towards higher wavenumbers.[24] Thus, on the basis of the considerations of Mozgawa,[24] the peak at 738 cm^{-1} can be attributed to the vibrations of the rings with a lower number of members, *e.g.* the simple four-membered ring (S4R), arising from the partial break-down of the zeolite A framework. It must be said that this assignment is not in agreement with the data reported by Djordievic *et al.*[30] in a recent paper concerning the structural study of celsian glass derived from a Ba-exchanged zeolite A containing a residual Na content of 0.8 wt%. These authors found an IR band at 707 cm^{-1} in the spectra of both Ba-exchanged zeolite A and the glass obtained by thermally treating the Ba-exchanged zeolite A sample at 860 °C for 3.5 hours and they related this band to the Al–O valence vibration.[30] This assignment does not appear to be consistent with the findings reported by Mozgawa[24] in the range (720–790 cm^{-1}) where the vibrational modes of the S4R in natural zeolites are active and with the results of Smirnov and Bougeard[29] which show that in the calculated IR spectrum of zeolite A no vibrations specific to AlO_4 units or Al–O bonds can be assigned. The structural rearrangement occurring during the exchange of $2Na^+$ with Ba^{2+} also involves the short-range order of the zeolitic structure with the formation of tetrahedra with non-bridging oxygens as the peak at 857 cm^{-1} shows. The comparable *I* values of these peaks, Table 1, further support this hypothesis that is also in good agreement with the XRD analysis previously reported.[19]

The peak fitting analysis of the FTIR spectra of the Ba-exchanged zeolite A thermally treated samples reveals that the transformations arising from the various thermal treatments affect both the short- and the middle-range order of the resulting structure (Table 1). As far as the tetrahedra inner structural order is concerned, the fitting shows that thermal treatments up to 500 °C gives rise to two considerable changes. The first concerns the characteristic peaks of the zeolite A structure[29] (1050, 995 and 938 cm^{-1} for the sample heated up to 200 °C and then quenched in air) which are connected with the stretching vibrations of the Si–O and Al–O bonds of the tetrahedra groups, which gradually shift toward the values 1078 ($I = 0.58$), 972 ($I = 0.57$) and 913 ($I = 0.46$) cm^{-1} for the sample heated up to 500 °C and then quenched in air. It is noteworthy that for this sample the two most intense absorption bands are very similar to the ones of the monoclinic polymorph of celsian (Fig. 3d). The second concerns the peak at about 850 cm^{-1}. Actually its estimated relative absorbance assumes a value almost constant for Ba-exchanged zeolite A samples thermally treated at 200, 300, 400 and 500 °C (0.13, 0.13, 0.14 and 0.11, respectively). This value is much higher than the homologous value exhibited by the Ba-exchanged zeolite A sample not thermally treated ($I = 0.044$). The transformations arising from the various thermal treatments of Ba-exchanged zeolite A affecting the middle range order of the resulting structure are clearly evidenced in Fig. 7, where the relative absorbance values of the three peaks lying in the range where there are active pseudolattice vibrations are plotted as a function of the temperature of the thermal treatment. From inspection of the data reported in Fig. 7 the following findings are evident.

1) Raising the temperature of the thermal treatment up to 500 °C results in a dramatic reduction in the estimated relative absorbance of the peak lying at about 570 cm^{-1}, which is related to the vibrational modes of the S6R units.

2) The estimated relative absorbance of the peak lying at about 680 cm^{-1}, related to the vibrational modes of the D4R units, increases from 0.15 (thermally untreated sample) to 0.35 (sample thermally treated at 400 °C) and then reaches 0.31 (sample thermally treated at 500 °C).

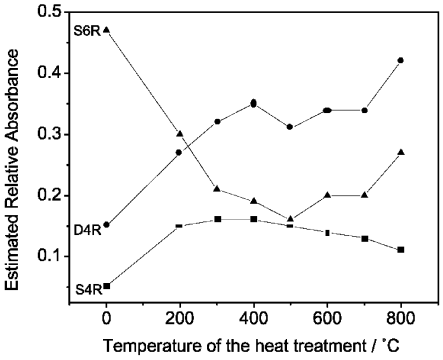

Fig. 7 Values of the estimated relative absorbance, I, for peaks corresponding to the vibrational modes of the S6R (▲), D4R (●), and S4R (■) units as a function of the temperature of thermal treatment.

3) The estimated relative absorbance of the peak corresponding to the S4R units, lying at about 740 cm^{-1}, assumes a value almost constant for Ba-exchanged zeolite A samples thermally treated at 200, 300, 400 and 500 °C (0.15, 0.16, 0.16 and 0.15, respectively). This value is much higher than the homologous value exhibited by the Ba-exchanged zeolite A sample not thermally treated ($I = 0.052$).

Thus the collapse of the microporous zeolitic structure resulting from the thermal treatment at 200 °C (Fig. 2a) also involves the partial disruption of the β cage structure forming tetrahedra rings with a lower number of members, while the local order appears unchanged, the exception being the increase in the amount of the depolymerised phase containing tetrahedra with non-bridging oxygens. Raising the temperature of the thermal treatment up to 400 °C gives rise to a fully amorphous aluminosilicate network (Figs. 2b and 2c) containing mostly double four-membered rings (D4R), whose microstructure progressively evolves toward the formation of a local order very similar to that of the monoclinic celsian. When the temperature of the thermal treatment is raised to 500 °C these structural transformations allow fast nucleation of the monoclinic polymorph followed by the growth of crystallites on a nanometric scale dispersed in the amorphous matrix (Fig. 2d). It should be emphasised that even if the monoclinic polymorph is thermodynamically stable in this temperature range, this transformation appears to be controlled mainly by kinetic factors under these conditions of thermal treatment. In this case the nucleation of monoclinic celsian, favoured by its structural similarity with the amorphous matrix, is followed by a very slow crystal growth.

As far as the phenomena occurring during the thermal treatments at temperatures higher than 500 °C are concerned, it is noteworthy that in the fitting of the FTIR spectra of the samples thermally treated at these temperatures, the peak at about 850 cm^{-1} disappears and, simultaneously, the position of the three peaks lying in the 800–1200 cm^{-1} range evolves in a different way as the temperature is varied (Table 1). Actually, when the temperature of the thermal treatment is raised to 800 °C, the peak at the highest wavenumber almost stays the same, whereas the locations of the second and third peak shift from 972 cm^{-1} ($I = 0.57$) and 913 cm^{-1} ($I = 0.46$) after the thermal treatment at 500 °C, to 1017 cm^{-1} ($I = 0.15$) and to 928 cm^{-1} ($I = 0.81$) after the thermal treatment at 800 °C, respectively. This last value is very similar to that of the highest absorption band of hexacelsian (934 cm^{-1}, Fig. 3c). Moreover it is noteworthy that, while in the temperature range of thermal treatment 500–800 °C, no appreciable structural variations in the long-range order were observed (Fig. 2d, 2e and 2f), significant changes in the medium-range order occur. Actually the trend in the estimated relative absorbance of the peaks corresponding to the vibrations of the S6R units undergoes a clear inversion starting from 500 °C and, thus begins to increase, while the one assigned to the D4R units goes on growing (Fig. 7). These results give strong indications that the amorphous matrix keeps on modifying upon heating from 500 to 800 °C, thus giving rise to a microstructure containing mainly D4R and S6R units characterized by a local order more similar to that of the hexagonal celsian. In other words, the rise in the temperature, instead of producing growth of the crystallites of monoclinic celsian previously formed at 500 °C, promotes mainly further evolution of the residual amorphous phase. This phenomenon is related to the fact that, in this temperature range, the growth of the monoclinic celsian crystals is far slower than the further transformation of the amorphous matrix. Therefore, in the subsequent stage of the thermal treatment (1000 °C), the microstructural environment required for the nucleation of the hexagonal polymorph occurs. It allows the growth of these crystallites, as shown by the XRD pattern of the sample heated up to 1000 °C, where the higher lines of the hexagonal celsian appear on the amorphous background with the pre-existing lines of the monoclinic polymorph (Fig. 2h). On the other hand this behaviour reflects the microstructural changes occurring in the amorphous matrix at this stage of the heat treatment. So the peak fitting of the FTIR spectrum of the Ba-exchanged zeolite A sample heated up to 1000 °C and then quenched in air exhibits three peaks in the 800–1200 cm^{-1} region (Table 1). The peak with the highest estimated relative absorbance ($I = 0.72$) as well as the peak with $I = 0.20$ occur at the same frequency as the main absorption bands of the FTIR spectrum of the hexagonal celsian polycrystalline sample (Fig. 3c), while the remaining one is detected at 1059 cm^{-1} ($I = 0.61$). Thus at this temperature, although the crystallization extent still appears low (Fig. 2h), the growth rate of hexacelsian becomes higher than the one of monoclinic celsian as a consequence of the fact that the microstructure of the residual amorphous phase progressively evolves toward the structure of hexacelsian. This transformation proceeds with an increase in the temperature and appears to be almost complete at 1300 °C, as shown by the XRD pattern of the polycrystalline sample shown in Fig. 1c.

It is noteworthy that this description of the microstructural evolution of the amorphous matrix with temperature is in good agreement with the one proposed by Djordjevic *et al.*[30] In fact these authors reported that the collapse of the microporous structure of the zeolite Ba-A starts with the breaking of Si–O–Al bridges within the D4R units, thus giving rise to an amorphous matrix. In this structure the presence of S6R units allows the occurrence of hexacelsian-like coordination which satisfies the Ba^{2+} coordination requirements.[30] On the basis of a reverse Monte Carlo simulation they proposed that the thermal treatment of the zeolite-derived glass for 1 h at 1100 °C results in the rearrangement of the tetrahedral framework into a layered structure from which hexacelsian crystallization is promoted.[30]

5 Conclusions

The use of FTIR spectroscopy has provided further insight into the thermal transformation of Ba-exchanged zeolite A to celsian. First of all it gave evidence that the partial breakdown of the zeolite structure arising from the exchange of $2Na^{+}$ with Ba^{2+} gave rise to the formation of S4R units. Secondly the use of FTIR spectroscopy allowed us to follow the evolution of the phases arising from the thermal collapse of the microporous structure of zeolite A. In particular it was found that in the 200–400 °C temperature range of thermal treatment a middle-range order of the amorphous phase occurs which favours the crystallisation of small crystallites of monoclinic celsian at 500 °C. Thirdly the use of FTIR spectroscopy gave evidence that the further evolution of the amorphous phase in the

500–800 °C temperature range of thermal treatment did not allow crystal growth of monoclinic celsian. Actually the sharp increase in this temperature range of the S6R units gave rise to a middle-range order more favourable to the crystallisation of hexacelsian which occurred on thermally treating the Ba-exchanged zeolite A sample to 1000 °C.

On the basis of these conclusions it should be noted that the heating up to 500 °C appears to be a singular stage in the thermal treatment. Actually it seems very interesting to investigate the possible changes occurring in the microstructure of the amorphous matrix when thermal treatments at this temperature are performed for longer periods of time, which could be the subject of a forthcoming paper.

On the whole the results of this investigation confirm the findings of ref. 19 and supply valid explanations for them. In particular the crystallisation of small aggregates of monoclinic celsian at 500 °C may be attributed to the reorganisation of the nanocrystalline fragments of zeolitic structure arising from the Ba-exchange and thermal collapse of the zeolite structure, whereas the crystallisation of hexacelsian at 1000 °C may be attributed to the evolution of the residual amorphous phase toward the hexacelsian whose crystallisation exhibits a lower kinetic barrier than monoclinic celsian.

Acknowledgement

This work was carried out with the financial contribution of the Ministry of University and Scientific and Technological Research, bando: COFIN 2000, protocollo: MM09071425.

References

1 I. G. Talmy, D. A. Haught and E. J. Wuchina, in *Proceedings of the 6th International SAMPE Electronic Conference*, Society for the Advancement of Materials and Process Engineering, ed. A. B. Goldberg and C. A. Harper, Covina, CA, USA, 1992, p. 687.
2 N. P. Bansal and C. H. Drummond III, *J. Am. Ceram. Soc.*, 1993, **76**(5), 1321.
3 N. P. Bansal, *J. Mater. Sci.*, 1998, **33**, 4711.
4 N. P. Bansal, *J. Am. Ceram. Soc.*, 1997, **80**(9), 2407.
5 N. P. Bansal, *US Pat.*, 5,214,004, May 25, 1993.
6 N. P. Bansal, *US Pat.*, 5,389,321, Feb 14, 1995.
7 N. P. Bansal, NASA TM 106993, Aug 1995.
8 N. P. Bansal, NASA TM 210216, Jun 2000.
9 J. Z. Gyekenyesi and N. P. Bansal, NASA TM 210214, Jul 2000.
10 G. Dell'Agli, C. Ferone, M. C. Mascolo and M. Pansini, *Solid State Ionics*, 2000, **127**, 309.
11 H. C. Lin and W. R. Foster, *Am. Mineral.*, 1962, **53**, 134.
12 M. Chen, W. E. Lee and P. F. James, *J. Non-Cryst. Solids*, 1991, **130**, 322.
13 B. Hoghooghi, J. McKittrick, E. Helsel and O. Lopez, *J. Am. Ceram. Soc.*, 1998, **81**(4), 845.
14 M. A. Subramanian, D. R. Corbin and R. D. Farlan, *Mater. Res. Bull.*, 1986, **21**, 1525.
15 U. V. Chowdry, D. R. Corbin and M. A. Subramanian, *US Pat.*, 4,813,303, 21 March 1989.
16 M. A. Subramanian, D. R. Corbin and U. V. Chowdry, *Adv. Ceram.*, 1989, **26**, 239.
17 D. R. Corbin, J. B. Parise, U. V. Chowdry and M. A. Subramanian, *Mater. Res. Symp. Proc.*, 1991, **233**, 213.
18 D. W. Breck, in *Zeolite Molecular Sieves: Structure, Chemistry and Use*, Wiley, New York, NY, 1974.
19 C. Ferone, G. Dell'Agli, M. C. Mascolo and M. Pansini, *Chem. Mater.*, 2002, **14**, 797.
20 G. Scwarzenbach and H. Flaschka, in *Complexometric Titration*, Methuen, London, 1969.
21 C. Baerlocher, W. M. Meier and D. H. Olson, in *Atlas of the Zeolite Framework Types*, Elsevier, Amsterdam, 2001.
22 A. Aronne, S. Esposito and P. Pernice, *Mater. Chem. Phys.*, 1997, **51**, 163.
23 W. Mozgawa, M. Sitarz and M. Rokita, *J. Mol. Struct.*, 1999, **511-512**, 251.
24 W. Mozgawa, *J. Mol. Struct.*, 2001, **596**, 129.
25 B. Yoshiki and K. Matsumoto, *J. Am. Ceram. Soc.*, 1951, **34**(9), 283.
26 T. Scanu, J. Guglielmi and Ph. Colomban, *Solid State Ionics*, 1994, **70/71**, 109.
27 D. W. Marquardt, *J. Soc. Ind. Appl. Math.*, 1963, **11**, 431.
28 A. M. Efimov, *J. Non-Cryst. Solids*, 1999, **253**, 95.
29 K. S. Smirnov and D. Bougeard, *J. Mol. Struct.*, 1995, **348**, 155.
30 J. Djordjevic, V. Dondur, R. Dimitrijevic and A. Kremenovic, *Phys. Chem. Chem. Phys.*, 2001, **3**, 1560.